
**LOW-DIMENSIONAL SYSTEMS
AND SURFACE PHYSICS**

Stability of Cubic Zirconia and of Stoichiometric Zirconia Nanoparticles

V. G. Zavodinsky and A. N. Chibisov

*Institute of Materials Science, Khabarovsk Scientific Center, Far East Division,
Russian Academy of Sciences, Khabarovsk, 680042 Russia
e-mail: vzavod@mail.ru*

Received December 15, 2004; in final form, April 29, 2005

Abstract—Using the electron density functional method, it is shown that the oxygen sublattice of cubic zirconia is unstable with respect to random displacements of oxygen atoms, which results in general instability of bulk cubic zirconia at low temperatures. A comparison of the equilibrium atomic structures and total energies of stoichiometric ZrO_2 nanoparticles about 1 nm in size shows that particles with cubic symmetry are more stable than those with rhombic (close-to-tetragonal) symmetry. The electronic structure of nanoparticles exhibits an energy gap at the Fermi level; however, this gap (depending on the symmetry and size of the particle) can be much narrower than the energy gap of the bulk material.

PACS numbers: D61.46.–w, 77.84.Bw

DOI: 10.1134/S1063783406020296

1. INTRODUCTION

Zirconia (ZrO_2) is a ceramic material; it has a number of interesting and useful properties and exists in three crystal phases. At temperatures below 1400 K, the monoclinic phase is thermodynamically stable; from 1400 to 2570 K, zirconia exists in a tetragonal phase; and, from 2570 K to the melting point (2980 K), it is cubic [1, 2].

Actually, both tetragonal and monoclinic phases are derivatives of the cubic phase, which has a fluorite structure. The tetragonal phase forms from the cubic phase through a specific reconstruction of the cubic oxygen sublattice (when half of the oxygen atoms are displaced with respect to the other half) and elongation of the unit cell in the direction of the displacement of oxygen atoms. The monoclinic phase forms from the tetragonal phase through a shear deformation of the entire unit cell with a variation in the lengths of its edges.

Although the cubic phase is the highest temperature phase, it has the greatest density and its energy is only slightly lower than that of the tetragonal phase: 0.052 eV per ZrO_2 formula unit [3].

Experiments [4] and calculations [5] show that the instability of the cubic phase is related to the tendency of the oxygen sublattice to become distorted along the $\langle 100 \rangle$ direction. The positions of oxygen atoms a_{O} along this direction can be expressed in terms of the distortion parameter d as

$$z_{\text{O}} = (0.25 + d)c,$$

where c is the lattice constant along the distortion direction and the quantity d can assume both positive and negative values.

The total energy of the crystal as a function of d has two minima (one at a positive and the other a negative value of d). The central position of oxygen atoms (at $d = 0$) corresponds to the ideal cubic structure and is unstable. Experimental and theoretical equilibrium values of d are equal to 0.065 and 0.052, respectively. It is shown in [6] that the distortion of the oxygen sublattice is characteristic not only of the tetragonal phase of zirconia but also of the cubic phase. The cubic structure becomes stable only at high temperatures, where oxygen atoms hop from one minimum to the other and, on the average, cubic symmetry is realized, since heavier zirconium atoms are too slow to follow the hopping of the oxygen atoms.

The cubic phase can be stabilized (i.e., its instability temperature can be lowered) by introducing additives, such as Mg, Ca, Fe, and Y. However, impurity-induced stabilization is accompanied by the appearance of numerous oxygen vacancies in ZrO_2 , thus drastically increasing its ionic electrical conductivity. One way of creating stable dielectric ceramics on the basis of high-temperature phases of zirconia is through their formation from nanoparticles. In recent years, studies on the preparation of stable thin films and nanoparticles from pure (undoped) zirconia with tetragonal [7–12] and cubic [13, 14] structures have been performed. It has been shown experimentally and theoretically that a tetragonal–cubic phase transition occurs at low tempera-

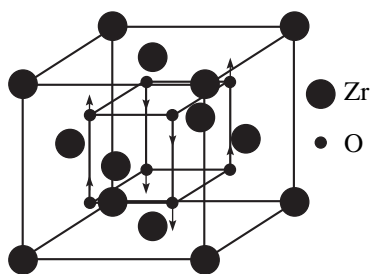


Fig. 1. Configuration of zirconium and oxygen atoms in a cell of cubic ZrO_2 (schematic). Arrows indicate the direction of displacements of oxygen atoms from the ideal cubic positions as a result of distortion.

tures in particles about 2 nm in size [15]. However, the theoretical results [15] were obtained disregarding the relaxation of the atomic structure of nanoparticles (i.e., these results apply to nonequilibrium states) and, therefore, cannot be considered sufficiently reliable.

The aim of the present study is to investigate the instability mechanism of the bulk cubic phase of zirconia, determine the reasons for the stability of ZrO_2 nanoparticles with cubic structure, and specify the energy and atomic structure of nanoparticles with tetragonal and cubic symmetry using computer simulation based on the *ab initio* quantum-mechanical approach.

2. METHOD AND CALCULATION DETAILS

Calculations were performed using the FH196MD software package [16] constructed on the basis of the electron density functional theory [17, 18] and the pseudopotential method. This package is an effective tool that has been used by many research groups to calculate the total energy of multiatomic systems (molecules, crystals, crystal defects, surfaces) for a wide class of materials. In particular, we used this software package previously to study the mechanism of ionic conduction in bulk zirconia [19]. To calculate the exchange and correlation energies, we used the gradient approximation in the form suggested by Perdew and Wang [20]. Pseudopotentials were constructed using the Troullier–Martins technique [21] and the FHI98PP computer program [22]; the calculated potentials were tested for the absence of ghost states and checked for the reproducibility of the main lattice characteristics of bulk materials (lattice constants and elastic moduli).

The cutoff energy for a set of plane waves was taken to be 44 Ry. As a minimum cell of bulk zirconia, a Zr_4O_8 cell (shown in Fig. 1) was used. In the cubic phase, all edges of this cell were identical ($a = b = c$) and the value $a = 0.522$ nm corresponded to the minimum of the total energy. When studying the cubic–tetragonal phase transition, we varied the parameters of the cell and searched for the minimum of the total

energy as a function of the set $\{a, b, c\}$. To study nanoparticles, we used supercells of such a size that the vacuum gaps between the particles ensured the absence of interaction between them. Since calculations were performed with standard personal computers with restricted technical capacities, the maximum size of the investigated nanoparticles was about 1 nm. In studying nanoparticles, one \mathbf{k} point (0, 0, 0) was used, and, for the simulation of bulk zirconia, two special points of the Brillouin zone were chosen, (0.25, 0.25, 0.25) and (0.25, 0.25, 0.75), with weights of 0.25 and 0.75, respectively. A similar approach is often applied to insulators and semiconductors when restricted computational resources do not allow use of a greater number of \mathbf{k} points.

3. RESULTS AND DISCUSSION

3.1. Distortion of Oxygen Atoms in Bulk Cubic Zirconium Dioxide

All atoms of the Zr_4O_8 cell were initially located in ideal cubic positions, with the lattice constant having the theoretical equilibrium value ($a = 0.522$ nm). Then, the total energy and the forces acting on the atoms were calculated self-consistently. The boundary atoms of the cell (Zr atoms) were fixed, while the oxygen atoms remained free. It appeared that the oxygen atoms were not displaced spontaneously from the ideal cubic positions (the forces acting on them were equal to zero). Attempts to transform the cubic cell into a tetragonal cell produced an increase in the total energy. Therefore, in the absence of displacements of the oxygen atoms (for example, at 0 K), the cubic lattice may be called quasi-stable. However, even a very small displacement of one oxygen atom (by 0.0001 nm) led to increasing displacements of half of the oxygen atoms in one direction and of the other half in the opposite direction. These displacements caused a distortion of the oxygen lattice in the $\langle 100 \rangle$ direction and resulted in nonzero forces on the atoms of the zirconium sublattice.

The appearance of nonzero forces acting on zirconium atoms indicates instability of the cubic cell at nonzero temperatures. To find the equilibrium shape of the cell, we changed its parameters (a, b, c) and found that the total energy of the system has a minimum when the cell is elongated in the direction in which the oxygen atoms are displaced (along the c axis) and is compressed in the two other directions with $a = b$. (We did not consider variations of the angles, i.e., the transition to the monoclinic phase). The ratio c/a was calculated to be 1.020, which is quite close to the value of 1.026 characteristic of the tetragonal phase. The calculated equilibrium distortion d for cubic ZrO_2 appeared to be equal to 0.045, which is close to the value of 0.052

obtained in [5] for the tetragonal phase. The average displacement of the oxygen atoms was 0.012 nm.

The instability of the oxygen sublattice of cubic zirconia with respect to small displacements of oxygen atoms was checked for a cell of greater size, $Zr_{32}O_{64}$. The effect remained the same as that for the Zr_4O_8 cell; namely, a displacement of one oxygen atom induces collective shifts of pairs of oxygen atoms in opposite directions with a distortion d of about 0.05 and the simultaneous appearance of nonzero forces acting on zirconium atoms.

Obviously, in ideal zirconia, all oxygen atoms are equivalent; therefore, at high temperatures, their tendency toward distortion leads to vibrations of oxygen sublattices with respect to each other and, in fact, with respect to their cubic equilibrium position. The heavier zirconium atoms are too slow to follow fast oscillations of the oxygen subsystem (which on the average remains cubic), and the system as a whole has cubic symmetry. Detailed analysis of the mechanism of the appearance of the high-temperature cubic phase of zirconia would require separate study.

3.2. Structure and Energy Characteristics of Nanoparticles

In contrast to [15], we concentrated on studying the stoichiometric particles of zirconia, since (as preliminary computations have shown [23]) stoichiometric particles are energetically more favorable than nonstoichiometric particles and have a dielectric electronic structure; i.e., there is a gap separating the occupied states from unoccupied states in their energy spectrum.

An analysis of the equilibrium geometry and energy characteristics of nanoparticles was performed for Zr_6O_{12} , $Zr_{10}O_{20}$, and $Zr_{14}O_{28}$ particles, which are fragments of the bulk lattice of cubic zirconia (Fig. 2).

The initial positions of the atoms in these particles correspond to the cubic phase; however, the symmetry of the particles is not cubic. The symmetry of these particles is that of a rectangular parallelepiped whose lateral surfaces are orthogonal to its bases; therefore, it is natural to expect that the internal equilibrium geometry of the particles (i.e., the relation between the inter-

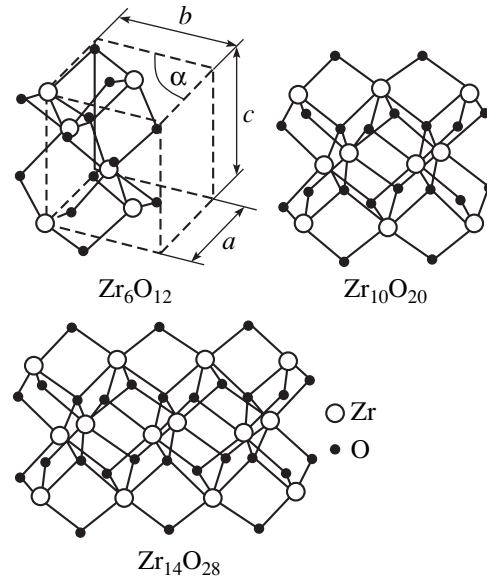


Fig. 2. Zr_6O_{12} , $Zr_{10}O_{20}$, and $Zr_{14}O_{28}$ nanoparticles. For the Zr_6O_{12} particle, dashed lines show the unit cell corresponding to the initial cubic phase ($a = b = c$, $\alpha = 90^\circ$).

atomic distances in different directions) will reflect the same symmetry, i.e., will change from cubic to tetragonal. The transition to monoclinic symmetry is also possible if the corresponding structure is energetically more favorable.

Our calculations showed that the relations $a = b = c$ and $\alpha = 90^\circ$ characteristic of the cubic phase are not satisfied if the atomic geometry of Zr_6O_{12} , $Zr_{10}O_{20}$, and $Zr_{14}O_{28}$ becomes equilibrium. For the smallest particle (Zr_6O_{12}), the parameter c exceeds a and b ($a = b = 0.460$ nm, $c = 0.488$ nm, $c/a = 1.062$), the angle α increases to 100° , and the base of the parallelepiped cell transforms from a square to a rhombus. The equality $a = b$ is also valid for $Zr_{10}O_{20}$ and $Zr_{14}O_{28}$ particles; however, the parameter c increases and the angle α decreases. Therefore, the symmetry of these nanoparticles is orthorhombic (intermediate between tetragonal and monoclinic).

In Table 1, the geometrical parameters of the Zr_6O_{12} , $Zr_{10}O_{20}$, and $Zr_{14}O_{28}$ particles are compared with the

Table 1. Calculated geometrical parameters of Zr_6O_{12} , $Zr_{10}O_{20}$, and $Zr_{14}O_{28}$ nanoparticles and analogous experimental data for the bulk tetragonal phase

Geometrical parameters	Zr_6O_{12}	$Zr_{10}O_{20}$	$Zr_{14}O_{28}$	Bulk tetragonal ZrO_2
a , nm	0.460	0.460	0.492	0.505
b , nm	0.460	0.460	0.492	0.505
c/a	1.062	1.080	1.093	1.026
α , deg	100	96	92	90
Particle size, nm \times nm \times nm	$0.32 \times 0.37 \times 0.78$	$0.68 \times 0.35 \times 0.75$	$0.99 \times 0.36 \times 0.76$	

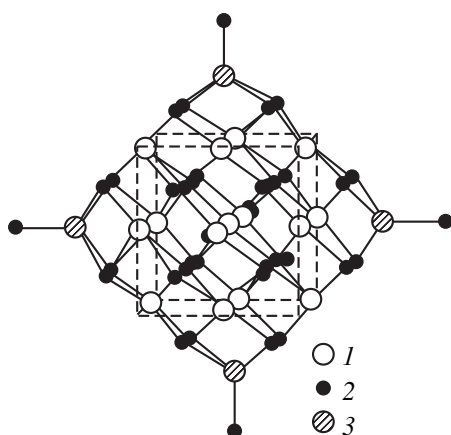


Fig. 3. Atomic configuration of a relaxed $Zr_{19}O_{38}$ nanoparticle (schematic): (1) zirconium atoms occupying the positions corresponding to bulk ZrO_2 , (2) oxygen atoms, and (3) zirconium atoms added for saturation of the bonds of the outer oxygen atoms (to ensure stoichiometry, one oxygen atom is added to each of these additional zirconium atoms). Dashed lines show a cubic cell with edge a .

experimental data for the bulk tetragonal phase. The parameters for the $Zr_{10}O_{20}$ and $Zr_{14}O_{28}$ particles are averaged, since their values are somewhat different inside a particle and at its edges. From Table 1, we see that the parameters of the nanoparticles approach their values for the tetragonal phase as the particles increase in size. It is significant that, in all cases, the lateral surfaces of the parallelepiped cells remain orthogonal to their bases; i.e., there is no tendency toward the appearance of monoclinic symmetry.

As noted above, it is not surprising that, for equilibrium Zr_6O_{12} , $Zr_{10}O_{20}$, and $Zr_{14}O_{28}$ particles, the relations between the geometrical parameters differ from those characteristic of the cubic phase; indeed, the symmetry of these particles is not initially cubic. In order to establish the features of the transitions between the cubic and noncubic phases more reliably, we need to study the relaxation of nanoparticles whose initial geometry is cubic. As an example, we considered a $Zr_{19}O_{38}$ particle, whose atomic configuration is shown in Fig. 3. It is a minimum stoichiometric particle with cubic symmetry which can be constructed for zirconia. Unfortunately, it was also the maximum particle that we could study using the available equipment.

The $Zr_{19}O_{38}$ particle was obtained by cutting a $Zr_{13}O_{32}$ cluster from the lattice of cubic zirconia and adding six zirconium atoms and six oxygen atoms to this cluster. We had to add zirconium and oxygen atoms for two reasons. First, in this way, the particle becomes stoichiometric and its electronic structure acquires dielectric character (there appears an energy gap at the Fermi level). Second, the bonding energy (per atom) decreases and the particle (with cubic symmetry) becomes more stable than the Zr_6O_{12} , $Zr_{10}O_{20}$, and $Zr_{14}O_{28}$ particles described above, whose geometry approaches that of the tetragonal phase. We believe that such particles can also form in real situations.

The optimization of the geometry showed that the symmetry of the $Zr_{19}O_{38}$ particle remains close to cubic after complete relaxation. The parameter a (the length of the edges of the cube shown by dashed lines in Fig. 3) becomes equal to 0.505 nm, which coincides with the experimental value of the cubic lattice constant but is smaller than the above theoretical equilibrium value (0.522 nm).

Table 2 lists the bonding energies E_b (per ZrO_2 formula unit) and the energy gaps ΔE for the nanoparticles of silicon dioxide we studied.

From comparing the data given in Table 2, it follows that a nanoparticle with cubic geometry is energetically more favorable than particles whose geometry is close to tetragonal. However, the energy gap for the Zr_6O_{12} , $Zr_{10}O_{20}$, and $Zr_{14}O_{28}$ particles is wider than that for the $Zr_{19}O_{38}$ particle. Apparently, the Zr_6O_{12} , $Zr_{10}O_{20}$, and $Zr_{14}O_{28}$ particles are almost undistorted fragments of the bulk lattice of zirconia and the saturation of the valence bonds in them is almost ideal. On the other hand, as noted above, the $Zr_{19}O_{38}$ particle contains edge atoms (Zr and O) whose positions do not correspond to those in the bulk material; i.e., they do not ensure the optimum bond saturation. Therefore, the energy gap (an analog of the band gap) for a cubic particle is narrower than that for a tetragonal particle.

We note that the positions of the oxygen atoms in the $Zr_{19}O_{38}$ particle do not correspond exactly to the ideal cubic positions. Therefore, when these atoms deviate from their equilibrium positions, the oxygen subsystem does not reveal a tendency toward distortion. In other words, the small distortion of cubic symmetry

Table 2. Calculated energy characteristics of zirconia nanoparticles

Energy characteristics	Rhombic (close-to-tetragonal) symmetry			Close-to-cubic symmetry	Bulk ZrO_2 (calculation)	
	Zr_6O_{12}	$Zr_{10}O_{20}$	$Zr_{14}O_{28}$	$Zr_{19}O_{38}$	this work	[24]
E_b , eV	-23.09	-23.49	-23.81	-24.15	-25.91	-26.20
ΔE , eV	2.5	2.7	2.6	1.5	3.5	3.07

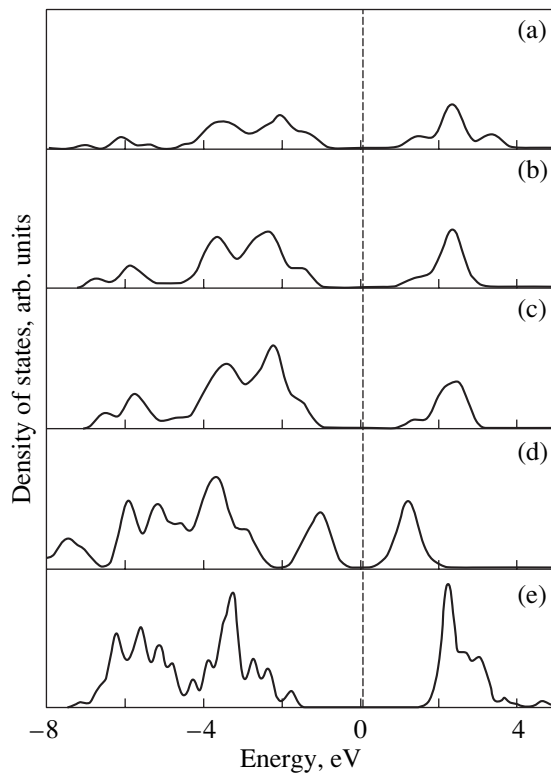


Fig. 4. Calculated electronic densities of states of (a) Zr_6O_{12} , (b) $\text{Zr}_{10}\text{O}_{20}$, (c) $\text{Zr}_{14}\text{O}_{28}$, and (d) $\text{Zr}_{19}\text{O}_{38}$ nanoparticles and (e) bulk cubic zirconia.

caused by the size effect stabilizes the close-to-cubic symmetry of the nanoparticle even in the absence of impurities.

The calculated energy gaps (even for bulk ZrO_2) are much smaller than the experimental value of 6 eV [25]. This feature is common for calculations based on the one-particle approximation [24]. As shown in [26], only by including many-particle effects can one obtain good agreement with experiment.

For a more complete comparison of the electronic structure of nanoparticles with that of bulk zirconia, we constructed the electronic density of states by replacing each electronic level with a 0.1-eV-wide Gaussian profile. The result is shown in Fig. 4. We see that, for the Zr_6O_{12} , $\text{Zr}_{10}\text{O}_{20}$, and $\text{Zr}_{14}\text{O}_{28}$ particles, the electronic density of states approaches that for bulk zirconia as the nanoparticles increase in size. However, for the $\text{Zr}_{19}\text{O}_{38}$ particle, which is larger than the Zr_6O_{12} , $\text{Zr}_{10}\text{O}_{20}$, and $\text{Zr}_{14}\text{O}_{28}$ particles, the electronic density of states is substantially different. As already noted, this circumstance can be explained by the fact that the Zr_6O_{12} , $\text{Zr}_{10}\text{O}_{20}$, and $\text{Zr}_{14}\text{O}_{28}$ particles are fragments of the structure of bulk zirconia, whereas the $\text{Zr}_{19}\text{O}_{38}$ particle contains additional atoms whose arrangement does not correspond to this structure. The difference between the

atomic structures leads to a difference in the electronic structures.

4. CONCLUSIONS

We have studied the equilibrium atomic structure of zirconia nanoparticles about 1 nm in size using the density functional theory and the pseudopotential method. We have shown that particles with cubic geometry are more stable than particles with rhombic (close-to-tetragonal) geometry. The electronic spectrum of all investigated nanoparticles has an energy gap at the Fermi level. However, on the whole, the electronic structure of the nanoparticles differs substantially from that of bulk zirconia.

ACKNOWLEDGMENTS

This study was supported by the Russian Foundation for Basic Research (project no. 04-02-97000) and the Presidium of the Far East Division of the Russian Academy of Science.

REFERENCES

1. R. Aldebert and J. P. Traverse, *J. Am. Ceram. Soc.* **68**, 34 (1985).
2. R. J. Ackermann, S. P. Garg, and E. G. Rauth, *J. Am. Ceram. Soc.* **60**, 341 (1977).
3. M. W. Finnis, A. T. Paxton, M. Methfessel, and M. van Schilfgarde, *Phys. Rev. Lett.* **81**, 5149 (1998).
4. G. Teufer, *Acta Crystallogr.* **15**, 1187 (1962).
5. H. J. F. Jansen and J. A. Gardner, *Physica B + C (Amsterdam)* **150**, 10 (1988).
6. R. Orlando, C. Pisani, and E. Stefanovich, *Phys. Rev. B: Condens. Matter* **45**, 592 (1992).
7. Z.-Q. Ji and J. M. Rigsbee, *J. Am. Ceram. Soc.* **84**, 2841 (2001).
8. N. Igawa and Y. Ishii, *J. Am. Ceram. Soc.* **84**, 1169 (2001).
9. P. Bouvier, E. Djurado, C. Ritter, A. J. Dianoux, and G. Lucazeau, *Int. J. Inorg. Mater.* **3**, 647 (2001).
10. N.-L. Wu, T.-F. Wu, and I. A. Rusakova, *J. Mater. Res.* **16**, 666 (2001).
11. T. Nguyen and E. Djurado, *Solid State Ionics* **138**, 191 (2001).
12. R. Gómez, T. Lopez, X. Bokhimi, E. Muñoz, J.L. Boldú, and O. Novaro, *J. Sol-Gel Sci. Technol.* **11**, 309 (1998).
13. S. Roy and J. Ghose, *Mater. Res. Bull.* **35**, 1195 (2000).
14. U. Martin, H. Boysen, and F. Frey, *Acta Crystallogr., Sect. B: Struct. Sci.* **49**, 400 (1993).
15. S. Tsunekawa, S. Ito, Y. Kawazoe, and J.-T. Wang, *Nano Lett.* **3** (7), 871 (2003).
16. M. Bockstedte, A. Kley, J. Neugebauer, and M. Scheffler, *Comput. Phys. Commun.* **107**, 187 (1997).
17. P. Hohenberg and W. Kohn, *Phys. Rev. [Sect. B]* **136**, B864 (1964).

18. W. Kohn, and L. J. Sham, Phys. Rev. [Sect A] **140**, A1133 (1965).
19. V. G. Zavodinsky, Fiz. Tverd. Tela (St. Petersburg) **46** (3), 441 (2004) [Phys. Solid State **46** (3), 453 (2004)].
20. J. P. Perdew and Y. Wang, Phys. Rev. B: Condens. Matter **33**, 8800 (1986).
21. N. Troullier and J. L. Martins, Phys. Rev. B: Condens. Matter **43**, 1993 (1991).
22. M. Fuchs and M. Scheffler, Comput. Phys. Commun. **119**, 67 (1999).
23. V. G. Zavodinsky and A. N. Chibisov, *Abstracts of Papers of the VIII Regional Conference on Semiconductors, Dielectrics, Metals, and Magnets, Vladivostok, Russia, 2004* (Vladivostok, 2004), p. 48 [in Russian].
24. G. Jomard, T. Petit, A. Pasturel, L. Magaud, G. Kresse, and J. Hafner, Phys. Rev. B: Condens. Matter **59**, 4044 (1999).
25. R. H. French, S. J. Glass, F. S. Ohuchi, Y.-N. Xu, and W. Y. Ching, Phys. Rev. B: Condens. Matter **49**, 5133 (1994).
26. B. Králik, E. K. Chang, and S. G. Louie, Phys. Rev. B: Condens. Matter **57**, 7027 (1998).

Translated by I. Zvyagin